J Mater Sci (2014) 49:4379–4386
DOI 10.1007/s10853-014-8137-z

Microwave absorption properties of carbon fibers with carbon coils of different morphologies (double microcoils and single nanocoils) grown on them

Lei Liu · Pingge He · Kechao Zhou · Tengfei Chen

Received: 25 November 2013 / Accepted: 3 March 2014 / Published online: 15 March 2014

Abstract Double-carbon microcoils and single-carbon nanocoils were selectively grown on the surface of carbon fibers (CFs) via decomposition of acetylene at the temperature of 680 °C using Ni and Ni/Al_2O_3 catalysts, respectively. The morphology and microstructure of the as-prepared carbon coils–CFs were studied by SEM and Raman spectra, and the microwave absorption properties were also examined. Different from the double-carbon microcoils, no catalyst is observed at the growth tip of single-carbon nanocoils. It is considered that the Ni/Al_2O_3 binary catalysts would induce base growth model where only one remaining side of the catalyst particle contributes to nanofiber's growth, resulting in the formation of single-carbon nanocoil. The single-carbon nanocoils–CFs composite shows lower complex permittivity, larger chirality admittance, as well as better microwave absorption properties than those of double-carbon microcoils–CFs. The maximum RL of the single-carbon nanocoils–CFs composite is −41.2 dB, and the bandwidth of RL less than −10 dB is up to 9.6 GHz, which are also better than those of other carbon nanomaterials in the literature.

Electronic supplementary material The online version of this article (doi:10.1007/s10853-014-8137-z) contains supplementary material, which is available to authorized users.

L. Liu · P. He · K. Zhou · T. Chen (✉)
National Key Laboratory for Powder Metallurgy, Central South University, Changsha 410083, China
e-mail: tengfei@csu.edu.cn

L. Liu
e-mail: liulei-tyr@163.com

P. He
e-mail: pingge326@163.com

K. Zhou
e-mail: zhoukechao@csu.edu.cn

Introduction

Due to the increased requirements of innovative electromagnetic (EM) shielding materials both in commercial and military applications, these materials with light weight, good chemical stability, wide absorption frequency, and strong absorption characteristics have attracted increasing attention in recent years [1, 2]. As an important class of electromagnetic shielding and absorbing materials, carbon-based materials [3], particularly, one-dimensional carbon materials such as carbon nanotubes (CNTs), carbon nanofibers (CNFs), and carbon fibers (CFs) have been extensively investigated owing to their excellent mechanical and electric properties [4, 5]. Unfortunately, because the characteristic impedance of these one-dimensional carbon materials is far away from that of free space (the impedance matching is poor), their shielding microwave is mainly ascribed to reflection rather than absorption.

It has been recognized that chiral materials have the potential to achieve perfect impedance matching due to the additional chiral admittance [6]. As a type of chiral materials obtained with relative ease, carbon coils are famous for their special helical structure, elastic mechanical property, and electromagnetic cross-polarizing ability. These characteristics make them as the most promising high-performance microwave absorption materials [7, 8]. In general, carbon coils are synthesized by catalytic chemical vapor deposition (CCVD) method using transition metals and their alloys as catalysts. It is shown that the morphology and quality of carbon coils depend on the CCVD condition [9–11], the catalyst composition [12], and even the substrate or support materials [13]. However, selective synthesis of carbon coils with designed helicity in large quantities still remains unsettled. The problems of

dispersion and handling nanoscale carbon coils are also an obstacle to the overall applications.

Recently, it has been demonstrated that combining carbon nanostructures like CNFs and CNTs with well-established microscale reinforcements (CFs) provided an effective approach to disperse well carbon nanomaterials for achievement of high-performance composites [14–16]. More importantly, incorporation of carbon coils with CFs would generate great interest compared with their counterpart linear CNFs since carbon coil is one type of allotropic CNFs, which has special structure and additional properties. Previously, we have prepared carbon coils–CFs hybrid by directly growing carbon coils on the surface of CFs, and demonstrated that the hybrid materials show good microwave absorption ability [17]. The carbon coils in the previous paper are mainly composed of double microcoils, including a few twist-shaped nanocoils. It is noted that the absorption properties of carbon coils are related to their coiling morphology or their chiral characteristic. Shen et al. [18] reported that the ratio of the helix radius to pitch had a greater influence on the microwave absorbing properties than the permittivity for carbon microcoils. Qi et al. [19] researched the microwave absorption properties of CNTs with different helicities and found that the CNTs with low helicity and short length show better microwave absorbing ability. In this article, double-carbon microcoils, purer, and more regular than that of Ref. [17], and single-carbon nanocoils were synthesized on the surface of CFs. The microwave absorption properties of the two kinds of hybrid materials were investigated and compared in the frequency range of 2–18 GHz.

Experimental

The first step involved coating the surface of CFs with catalyst nanoparticles by a homogeneous precipitation method utilizing urea hydrolysis, which is similar to that previously reported in Ref. [17]. $Ni(NO_3)_2$ and $Ni(NO_3)_2$/$Al(NO_3)_3$ were chosen as the catalyst precursors. The molar ratio of Ni to Al was maintained at 3/1, and the total metallic ion concentration was maintained at 0.1 mol/L. After calcination and reduction, two kinds of catalyzed CFs, Ni-coated CFs and Ni/Al_2O_3-coated CFs, were obtained. The second step was to synthesize the carbon coils. A graphite chamber that is 25 cm in diameter and 50 cm in length was used as the reactor in a vertical furnace (equipped with temperature and gas-flow controls). The pyrolysis of acetylene (1 L/min) was conducted at 680 ± 5 °C for 1 h at atmospheric pressure. 1 L/min of H_2 (bubbled through thiophene) and 1 L/min of N_2 were used as dilute gases, in contrast to the previous paper [17] in which only H_2 was used as dilute gas.

The composition of catalyst was analyzed using energy dispersive X-ray spectroscopy (EDS) in the scanning electron microscopy (SEM). The morphology and structure of synthesized carbon products were investigated by SEM and Raman spectroscopy, respectively. The electromagnetic parameters of the samples, i.e., the relative complex permittivity ($\varepsilon_r = \varepsilon' - j\varepsilon''$) and permeability ($\mu_r = \mu' - j\mu''$), were measured by a transmission/reflection coaxial method in the range of 2–18 GHz using an E8363B PNA Series Network Analyzer. The testing specimens of cylindrical, toroidal-shaped samples (out = 7 mm, in = 3 mm) were fabricated by uniformly dispersing 10 wt % of the as-prepared carbon products (cut into short fibers with length about 1–2 mm) into wax. The reflection loss (RL) curves were calculated according to transmission line theory, as follows:

$$Z_{in} = \sqrt{\frac{\mu_r}{\varepsilon_r}} \tanh\left(j\frac{2\pi f d\sqrt{\mu_r \varepsilon_r}}{c}\right) \quad (1)$$

$$RL = 20\log\left|\frac{Z_{in}-1}{Z_{in}+1}\right| \quad (2)$$

where f is the frequency of electromagnetic wave, d is the thickness of the absorber, c is the velocity of light, and Z_{in} is the input impedance of the absorber.

Results and discussion

Characterization of catalyzed CFs

The EDS patterns and SEM (scanning electron microscopy) images of the two kinds of catalyzed CFs are shown in Fig. 1. A large number of nanoparticles were dispersed uniformly on the surface of CFs. The results of EDS analysis show the presence of C, Ni, and O in the Ni-coated CFs (Fig. 1a) and C, Ni, Al, and O in the Ni/Al_2O_3-coated CFs (Fig. 1b). The nanoparticles act as "seeds" in inducing carbon deposition, thus forming carbon coils. For the growth of carbon coils on CFs, it is very important to control the synthesis of "seeds" with desired size and uniform dispersion on the surface of CFs. The homogeneous precipitation method used in this paper gives good control over the precipitated nanoparticles. This can be attributed to the fact that homogeneous precipitation is carried out by introducing ammonia uniformly throughout the solution at the molecular levels, which is achieved by thermal decomposition of urea [20].

Morphologies and microstructures of carbon coils grown on CFs

The SEM images of carbon coils growing on Ni-coated CFs in different magnified views are shown in Fig. 2.

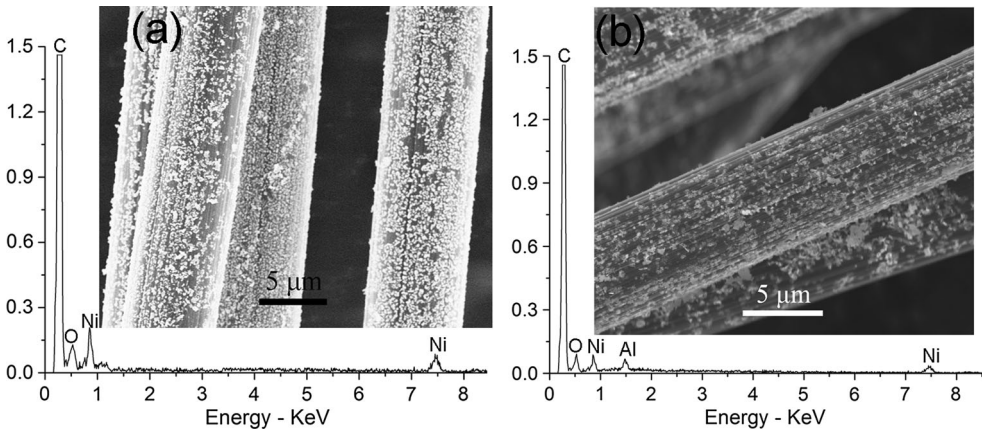

Fig. 1 EDS and SEM images of catalyzed CFs: **a** Ni-coated CFs, **b** Ni/Al_2O_3-coated CFs

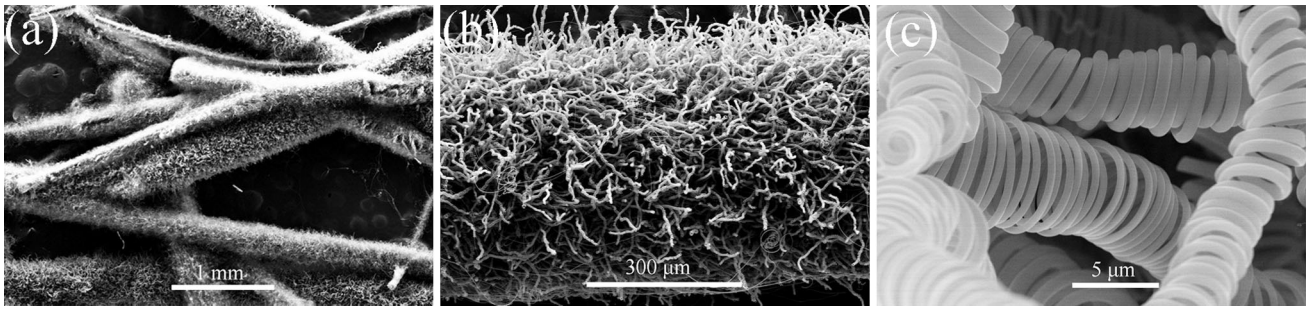

Fig. 2 SEM images of carbon coils grown on Ni-coated CFs: **a** general morphology, **b** typical image of a CF with double-carbon microcoils growth, and **c** higher magnification view of the double-carbon microcoils

The general morphology of the sample is shown in Fig. 2a, the typical image of a CF with carbon coils grown on them is shown in Fig. 2b, while a higher-magnification image of these carbon coils is shown in Fig. 2c. It explicitly shows that carbon coils were uniformly and densely grown on the surface of CFs. Compared with the previously reported carbon coil–CF hybrids [17], the carbon coils produced currently are almost pure double-carbon microcoils with higher regularity. The difference between the previous and current synthesis conditions is whether the nitrogen was introduced or not as dilute gas. It seems that a fraction of nitrogen significantly improved the growth selectivity of double-carbon microcoils. Unlike hydrogen gas, nitrogen did not decompose and participate in reaction during the CCVD. However, the concentration of reaction gas was diluted, and the gas residence time was shortened by introduction of nitrogen. All of these factors would determine the kind of hydrocarbon intermediates being formed and also influence the catalyst's characterization. As a result, the carbon coil yield and morphology would be remarkably affected by the nitrogen gas.

Figure 3 demonstrates the morphology of carbon coils growing on Ni/Al_2O_3-coated CFs. Apparently, carbon coils covered evenly and formed a network-like structure around the CFs (Fig. 3a and b). From the enlarged view, it is observed that most of them have single-helix structure that one nanofiber coiled to form a spring-like carbon nanocoil (Fig. 3c). These carbon coils can be defined as single-carbon nanocoils [21] to be distinguished from the double-carbon microcoils.

Figure 4 gives the comparison of SEM images of the double-carbon microcoils and single-carbon nanocoils. TEM image is also shown in the supplementary material (Fig. S1). It can be seen that in double-carbon microcoils (Fig. 4a), a catalyst grain appears on the coil tip, and two nanofibers originated from different sides or different crystal faces of the catalyst grain in an opposite direction, and then continuously cured and entwined in the same direction to form the double coil. The diameter of the nanofiber by which the double coil was built is about 250 nm, and the coil diameter ranged from 4 to 6 μm. On the contrary, in single-carbon nanocoils, no catalyst particle is observed at the coil tip, and only one nanofiber entwined to form a spring-like coil. In the middle of the nanofiber by which a coil was built, a groove is clearly observed on the surface (Fig. 4b). It seems that the nanofiber is formed by two fibers which adherently combined or fused with each other. The diameter of the nanofiber ranges from 100 to 150 nm, and the coil diameter is about 500 nm. The coil pitch of the single-carbon nanocoils is

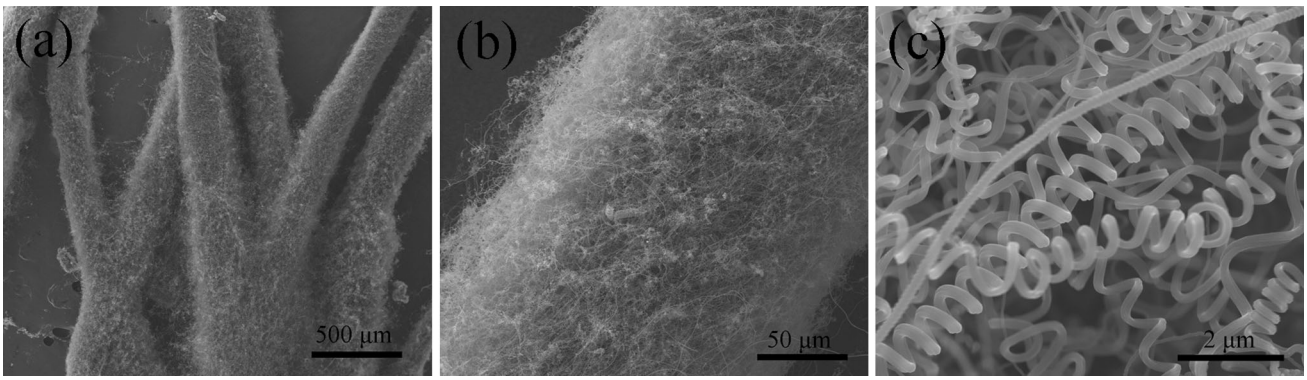

Fig. 3 SEM images of carbon coils growth on Ni/Al_2O_3-coated CFs: **a** general morphology, **b** typical image of a CF with single-carbon nanocoils growth, and **c** higher magnification view of the single-carbon nanocoils

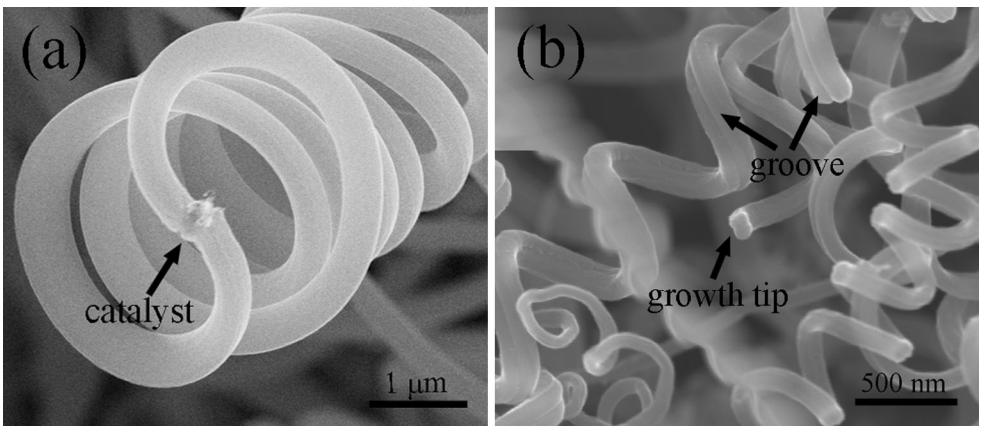

Fig. 4 SEM images of **a** the growth tip of double-carbon microcoil and **b** the growth tip of single-carbon nanocoil

generally the same as the coil diameter in size, while the coil pitch of the double-carbon microcoils is nearly zero. Chen et al. [22] considered that the larger coil pitch makes the mechanical and electric properties of spring-like single-carbon nanocoils more sensitive to the applied external energies such as mechanical and electric fields than those of double-carbon microcoils. Accordingly, the single-carbon coils are expected to be more novel and excellent sensor and have potential applications in Micro Electro Mechanical Systems, etc. Furthermore, it is recognized that the maximum chirality admittance achieved when the ratio of the helix radius "a" to pitch "p" is about 0.23 [23]. The greater the chirality admittance, the better the microwave absorption property achieved. The ratio a/p of the single-carbon nanocoils is about 0.5 which is adjacent to the value of maximum admittance 0.23, while the ratio a/p of the double-helix carbon microcoils should be too high because of their larger helix radius and nearly zero pitch. In this regard, single-carbon nanocoils should have better microwave absorption property than that of double-carbon microcoils.

In previous research works, using Fe–Ni–In- [12], and Fe–Cr-containing alloys [21] (stainless steel series) as catalysts, single-carbon nanocoils, morphology of which is similar to those described here, were also obtained in high yield. However, using pure Ni catalyst or high Ni content alloy catalyst, double-carbon microcoils with two nanofibers grown from two sides of a catalyst grain are mainly produced [23]. Although Chen et al. [22] synthesized single nanocoils over the Ni catalyst, they considered that the Fe impurity in molecular sieve supporter may poison, restraining one side of the catalyst grain and resulting in a monodirectional growth mode. In the present work, the morphology of carbon coils switched from double microcoils to single nanocoils with the addition of a trace amount of Al_2O_3 impurity in the Ni catalyst. Different from the double-carbon microcoils and the previously reported single-carbon nanocoils, no catalyst is observed at the growth tip of the single-carbon nanocoils synthesized in this paper. It may be postulated that the Ni/Al_2O_3 binary catalysts would have strong interaction with the CF substrate, resulting in base growth model of the carbon nanocoils. In

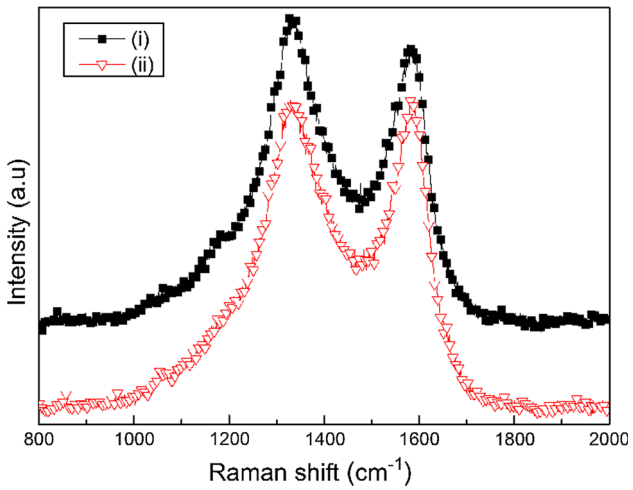

Fig. 5 Raman spectra of the double-carbon microcoil-coated CFs (*i*), and single-carbon nanocoil-coated CFs (*ii*)

this model, one side of the catalyst particle attached to the CF and only one nanofiber grew from the remaining side, contributing to the formation of single-carbon nanocoil. Moreover, Al_2O_3 would have an electronic interaction with the Ni catalyst and exert a profound effect on its oxidation states. According to the proposition of Dijon et al. [24] oxidation of the catalyst is necessary to induce the base growth mode of the CNTs. They also found that on Al_2O_3 substrate, Fe catalyst is fully oxidized inducing the base growth mode. However, the relationship between the catalyst composition and the morphology of the carbon coils should be further studied.

The Raman spectra of the double-carbon microcoil–CFs and single-carbon nanocoils–CFs are shown in Fig. 5. Two main peaks are exhibited in the Raman spectra: one is around 1330 cm^{-1} known as D-band originating from the disorder structure in carbon materials, and the other is around 1580 cm^{-1} known as G-band resulting from crystalline graphite structure. A strong peak of D-band and a broad peak of G-band in the spectrum indicate the presence of a large number of defects in the carbon coils and the amorphous structure of the carbon coils. However, the ration of I_D/I_G (1.1) corresponding to the single-carbon nanocoils is smaller than that of double-carbon microcoils (1.3), indicating that there are more graphite structures in the single nanocoils.

Microwave properties of the CFs with carbon coils grown on them

Figure 6 shows the complex permittivity real part (ε'), imaginary part (ε''), complex permeability real part (μ'), and imaginary part (μ'') of the composite A and B corresponding to the wax composites containing the double-helix carbon microcoils–CFs and single-carbon nanocoils-CFs, respectively. For the composite A (Fig. 6a), it can be seen that the ε' value decreases from 13.9 to 7.4 with the increasing frequency, while the ε'' value fluctuates between 6.8 and 4.5. Figure 6b displays the electromagnetic parameters of composite B showing that a resonant peak is around 10 GHz in the ε' and ε'' values. The ε' value is in the range of 7.7–3, and the ε'' value is in the range of 3.8–1.8. In comparison, both the ε' and ε'' values of composite B are lower than those of composite A. Moreover, due to the low-magnetic catalyst content, the μ' values of both A and B composites are slightly higher than 1, and the μ'' values are close to 0, concluding that the reflection loss (RL) should be mainly a result of dielectric loss. It should be noted that in the case of dielectric-loss absorbers, the lower permittivity is advantageous in terms of striking a balance between permeability and permittivity, which would lead to better impedance match and result in lower reflection coefficient [25]. Figure 7 exhibits the dielectric tangent loss ($\tan\delta_e = \varepsilon''/\varepsilon'$) of the two composites. It is observed that the $\tan\delta_e$ value of composite A fluctuates and increases from $\sim$0.5 to $\sim$0.7 with the rising frequency. While the $\tan\delta_e$ value of composite B is relatively low (less than 0.4) in the lower frequency range (2–7 GHz), the $\tan\delta_e$ value is higher than 0.5 after 8 GHz. One can also see a resonant peak around 10 GHz corresponding to the resonant peak in ε' and ε'' values.

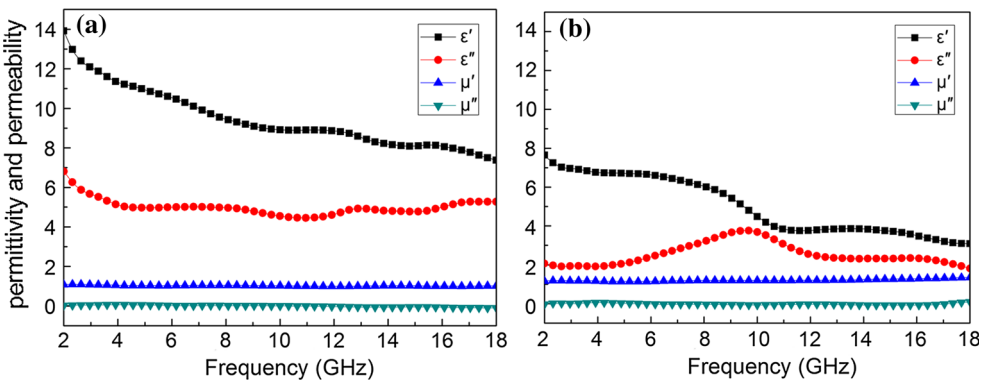

Fig. 6 Frequency dependences of real and imaginary parts of complex permittivity and permeability of the wax composites containing the double-carbon microcoils–CFs (**a**), and single-carbon nanocoils–CFs (**b**)

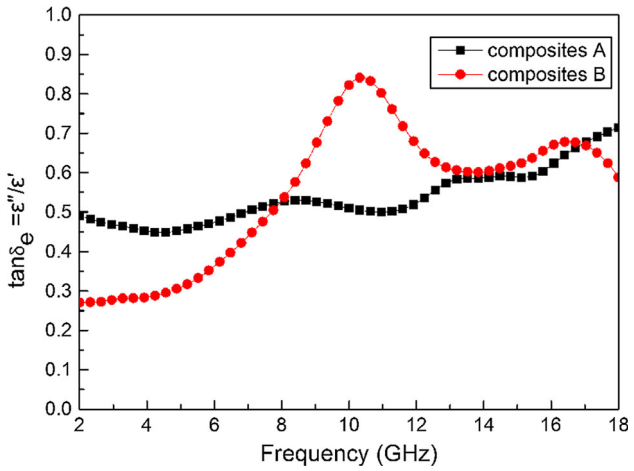

Fig. 7 Dielectric tangent loss ($\tan\delta_e$) of the composites

The reflection loss (RL) curves of the wax composites calculated using Eqs. (1) and (2) are shown in Fig. 8. Obviously, both the composites A and B exhibit good microwave absorption ability, and the RL values shift to lower frequency with the increasing thickness, suggesting that the range of absorption frequency can be modulated by adjusting the composite thickness. In detail, the composite A (Fig. 8a) exhibits the largest RL of −20.2 dB at 10.2 GHz for the composite thickness of 2.5 mm and the widest bandwidth of below −10 dB in the range of 11.1–15.6 GHz (bandwidth = 4.5 GHz) for 2.0 mm in thickness. By contrast, the composite B (Fig. 8b) has the optimal RL value of −41.2 dB at 8.5 GHz when the composites thickness is 3.5 mm, and its maximum bandwidth of absorption exceeding −10 dB is 9.6 GHz in the range of 8.4–18 GHz for 3 mm of thickness. It is also found that the absorption peaks of composite B are at the higher frequency compared to those of composite A. The microwave absorption ability of composite B is weaker than that of composite A in the lower frequency range, resulting from the low $\tan\delta_e$ value. However, the property of composite B as a whole is superior to that of composite A in the frequency range of 2–18 GHz. The better microwave absorption property confirms the expected better impedance matching of the single-carbon nanocoils due to the lower complex permittivity value and greater chirality admittance. The chirality admittance of the single-carbon nanocoils should also be greater than that of the helical carbon nanofibers with twist form, which were synthesized using Ni–Sn–O catalyst as described in Ref. [25]. Further, the single-carbon nanocoils exhibit better microwave absorption property than that of helical carbon nanofibers especially in the bandwidth less than −20 dB. The bandwidth of RL values less than −20 dB of single-carbon nanocoils is about 5.1 GHz with thickness in the range of 2.0–3.5 mm, while that of the helical carbon nanofibers is about 2.2 GHz. Compared to materials such as carbon nanobelts [26], helical carbon nanotubes [19], twin carbon nanocoils [27], etc., (Table 1), single-carbon coils–CFs are also outstanding. Moreover, the bandwidth of RL below −10 dB (9.6 GHz) is even wider than that of magnetic metal and oxide/carbon nanomaterials in the literature [2, 28–30] (Table 1). Therefore, the single-carbon coils–CFs obtained in this work are attractive candidates for the new type of microwave absorption materials with lightweight, good chemical stability, strong, and wide band absorption.

Conclusions

In summary, two kinds of carbon coils, double-carbon microcoils and single-carbon nanocoils, were synthesized on the surface of CFs by CCVD method using Ni and Ni–Al_2O_3 as catalysts, respectively. Two coiling nanofibers originated from different sides of the Ni nanograin which usually forms on the growth tip of double-carbon microcoils. However, no catalyst is observed at the growth tip of single-carbon nanocoil. It is considered that the Ni/Al_2O_3 binary catalysts would induce base growth model where only one remaining side of the catalyst grain contributes to nanofiber growth, resulting in the formation of single-carbon nanocoil. The ratio $a/p \sim 0.5$ of single-carbon

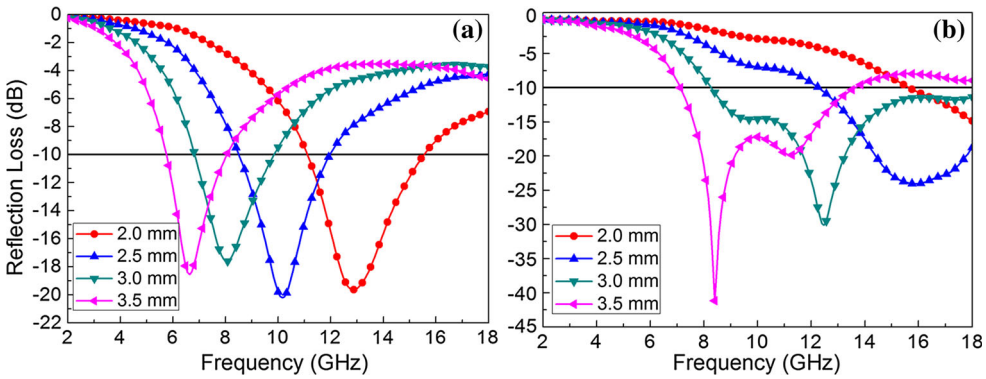

Fig. 8 Reflection loss curves of the wax composites containing the double-carbon microcoils–CFs (**a**), and single-carbon nanocoils–CFs (**b**)

Table 1 Microwave absorption performances of representative carbon nanomaterials composites

Samples in matrices	wt%	Max RL value (dB)	*d* (mm) (RL > 10 dB)	Frequency range (GHz) (RL > 10 dB)	Effective bandwidth (RL > 10 dB)	Refs.
Carbon nanobelts in wax	30	21.02	7.5	3.5–4.4, 11.2–13.6	3.3	[26]
Low helicity carbon nanotubes in wax	30	25.78	2	9.2–12.8	3.6	[19]
Twin carbon nanocoils in wax	15	36.09	2.5	10.5–16.93	6.43	[27]
Porous carbon/Co in wax	30	40	2.5	8–10.5	2.5	[28]
Fe_3O_4/Al_2O_3/CNCs in wax	25	28.3	2	10.5–14.0	3.5	[29]
Ni/graphene in wax	20	16	1.5	7.2–12.2	5	[2]
Fe@CNT in epoxy resin	10	31.71	1	11.8–14.7	2.9	[30]
HCNF-coated-CFs in wax	15	32	2.5	8.2–18	9.8	[25]
Double-carbon microcoils–CFs in wax	10	20.2	2.0	11.1–15.6	4.5	This work
Single-carbon nanocoils–CFs in wax	10	41.2	3.0	8.4–18	9.6	This work

nanocoils is more adjacent to the value of maximum admittance 0.23 than that of double-carbon microcoils, while the complex permittivity value of single-carbon nanocoils–CFs composite is lower than that of double-carbon microcoils–CFs composite. For lower complex permittivity and larger chirality admittance resulting in better impedance matching, the single-carbon nanocoils–CFs composite shows better microwave absorption property wherein maximum RL and the bandwidth of RL less than −10 are −41.2 dB and up to 9.6 GHz, respectively.

Acknowledgements This research was funded by Chinese Ministry of Science and Technology '863' Grant No. 2012AA03A207.

References

1. Kim JB, Lee SK, Kim CG (2008) Comparison study on the effect of carbon nano materials for single-layer microwave absorbers in X-band. Compos Sci Technol 68:2909–2916. doi:10.1016/j.compscitech.2007.10.035
2. Fang J, Zha W, Kang M, Lu S, Cui L, Li S (2013) Microwave absorption response of nickel/graphene nanocomposites prepared by electrodeposition. J Mater Sci 48:8060–8067. doi:10.1007/s10853-013-7600-6
3. Chung DDL (2001) Electromagnetic interference shielding effectiveness of carbon materials. Carbon 39:279–285. doi:10.1016/S0008-6223(00)00184-6
4. Cao MS, Song WL, Hou ZL, Wen B, Yuan J (2010) The effects of temperature and frequency on the dielectric properties, electromagnetic interference shielding and microwave-absorption of short carbon fiber/silica composites. Carbon 48:788–796. doi:10.1016/j.carbon.2009.10.028
5. Tellakula RA, Varadan VK, Shami TC, Mathur GN (2004) Carbon fiber and nanotube based composites with polypyrrole fabric as electromagnetic absorbers. Smart Mater Struct 13:1040–1044. doi:10.1088/0964-1726/13/5/009
6. Jaggard D, Engheta N (1989) Chirosorb as an invisible medium. Electron Lett 25:173–174. doi:10.1049/el:19890126
7. Motojima S, Hoshiya S, Hishikawa Y (2003) Electromagnetic wave absorption properties of carbon microcoils/PMMA composite beads in W bands. Carbon 41:2658–2660. doi:10.1016/S0008-6223(03)00292-6
8. Motojima S, Noda Y, Hoshiya S, Hishikawa Y (2003) Electromagnetic wave absorption property of carbon microcoils in 12–110 GHz region. J Appl Phys 94:2325–2330. doi:10.1063/1.1589603
9. Chen XQ, Motojima S (1999) The growth patterns and morphologies of carbon micro-coils produced by chemical vapor deposition. Carbon 37:1817–1823. doi:10.1016/S0008-6223(99)00054-8
10. Chen XQ, Yang SM, Kato Y, Motojima S (2007) Influence of CVD conditions on the growth of carbon microcoils with circular cross-sections. Mater Lett 61:2900–2903. doi:10.1016/j.matlet.2006.11.093
11. Li DW, Pan LJ, Wu YK, Peng W (2012) The effect of changes in synthesis temperature and acetylene supply on the morphology of carbon nanocoils. Carbon 50:2571–2580. doi:10.1016/j.carbon.2012.02.015
12. Yang S, Chen X, Motojima S (2004) Morphology of the growth tip of carbon microcoils/nanocoils. Diam Relat Mater 13:2152–2155. doi:10.1016/j.diamond.2004.06.014
13. Yang S, Chen X, Katsuno T, Motojima S (2007) Controllable synthesis of carbon microcoils/nanocoils by catalysts supported on ceramics using catalyzed chemical vapor deposition process. Mater Res Bull 42:465–473. doi:10.1016/j.materresbull.2006.06.026
14. Gong QM, Li Z, Zhou XW, Wu JJ, Wang Y, Liang J (2005) Synthesis and characterization of in situ grown carbon nanofiber/nanotube reinforced carbon/carbon composites. Carbon 43:2426–2429. doi:10.1016/j.carbon.2005.04.024
15. Mathur RB, Chatterjee S, Singh BP (2008) Growth of carbon nanotubes on carbon fibre substrates to produce hybrid/phenolic composites with improved mechanical properties. Compos Sci Technol 68:1608–1615. doi:10.1016/j.compscitech.2008.02.020
16. Zhang QH, Liu JW, Sager R, Dai LM, Baur J (2009) Hierarchical composites of carbon nanotubes on carbon fiber: influence of growth condition on fiber tensile properties. Compos Sci Technol 69:594–601. doi:10.1016/j.compscitech.2008.12.002
17. Liu L, Zhou K, He P, Chen T (2013) Synthesis and microwave absorption properties of carbon coil-carbon fiber hybrid materials. Mater Lett 110:76–79. doi:10.1016/j.matlet.2013.07.131
18. Shen ZM, Ge M, Zhao DL (2005) The microwave absorbing properties of carbon microcoils. New Carbon Mater 20:289–293. doi:10.3321/j.issn:1007-8827.2005.04.001
19. Qi XS, Yang Y, Zhong W, Deng Y, Au CT, Do YW (2009) Large-scale synthesis, characterization and microwave absorption

properties of carbon nanotubes of different helicities. J Solid State Chem 182:2691–2697. doi:10.1016/j.jssc.2009.07.036
20. Yu ZX, Chen D, Totdal B, Holmen A (2005) Effect of catalyst preparation on the carbon nanotube growth rate. Catal Today 100:261–267. doi:10.1016/j.cattod.2004.09.060
21. Yang SM, Chen XQ, Motojima S, Ichihara M (2005) Morphology and microstructure of spring-like carbon micro-coils/nano-coils prepared by catalytic pyrolysis of acetylene using Fe-containing alloy catalysts. Carbon 43:827–834. doi:10.1016/j.carbon.2004.11.014
22. Chen X, Takeuchi K, Yang S, Motojima S (2006) Morphology and growth mechanism of single-helix spring-like carbon nanocoils with laces prepared using Ni/molecular sieve (Fe) catalyst. J Mater Sci 41:2351–2357. doi:10.1007/s10853-006-7078-6
23. Ge F, Zhu J, Chen L (1996) Effective electromagnetic and chiral parameters of chiral composite material. Int J Infrared Milli 17:449–455. doi:10.1007/BF02088166
24. Dijon J, Szkutnik PD, Fournier A, de Monsabert TG, Okuno H, Quesnel E, Muffato V, De Vito E, Bendiab N, Bogner A, Bernier N (2010) How to switch from a tip to base growth mechanism in carbon nanotube growth by catalytic chemical vapour deposition. Carbon 48:3953–3963. doi:10.1016/j.carbon.2010.06.064
25. Liu L, He PG, Zhou KC, Chen TF (2013) Microwave absorption properties of helical carbon nanofibers-coated carbon fibers. AIP Adv. doi:10.1063/1.4818495
26. Qi XS, Yang Y, Zhong W, Qin CA, Deng Y, Au CT, Du YW (2010) Simultaneous synthesis of carbon nanobelts and carbon/Fe–Cu hybrids for microwave absorption. Carbon 48:3512–3522. doi:10.1016/j.carbon.2010.05.047
27. Tang N, Zhong W, Au C, Yang Y, Han M, Lin K, Du Y (2008) Synthesis, microwave electromagnetic, and microwave absorption properties of twin carbon nanocoils. J Phys Chem C 112:19316–19323. doi:10.1021/Jp808087n
28. Liu QL, Zhang D, Fan TX (2008) Electromagnetic wave absorption properties of porous carbon/Co nanocomposites. Appl Phys Lett. doi:10.1063/1.2957035
29. Wang GZ, Gao Z, Tang SW, Chen CQ, Duan FF, Zhao SC, Lin SW, Feng YH, Zhou L, Qin Y (2012) Microwave absorption properties of carbon nanocoils coated with highly controlled magnetic materials by atomic layer deposition. ACS Nano 6:11009–11017. doi:10.1021/Nn304630h
30. Zhao DL, Li X, Shen ZM (2009) Preparation and electromagnetic and microwave absorbing properties of Fe-filled carbon nanotubes. J Alloy Compd 471:457–460. doi:10.1016/j.jallcom.2008.03.127